ADVANCES IN MATERIALS SCIENCE, Vol. 24, No. 4 (82), December 2024

sciendo

DOI: 10.2478/adms-2024-0022

D. Elil Raja[1]*, S. Vijayan[2], Tushar Sonar[3], S. Prathap Singh[1]

[1]Department of Mechanical Engineering, St. Joseph's Institute of Technology, Chennai, Tamilnadu, India
[2]Department of Mechanical Engineering, Sri Sivasubramaniya Nadar College of Engineering, Chennai, Tamilnadu, India
[3]Department of Welding Engineering, Institution of Engineering and Technology, South Ural State University, Chelyabinsk, Russia

* *elilraja76@gmail.com*

ANALYZING THE DRY SLIDING WEAR PERFORMANCE ON ALUMINUM 6061 ALLOY REINFORCED WITH SiC AND B_4C HYBRID NANOCOMPOSITE

ABSTRACT

The methodology of enhancing the wear resistance of hybrid Metal Matrix Composites (MMCs) involves reinforcing the metal or alloy with robust materials. This study focuses on the manufacturing of a hybrid nanocomposite, which includes 0.6 vol.% of Silicon Carbide (SiC) and 0.2 vol.% of Boron Carbide (B_4C) nanoparticles with aluminum (Al) 6061 alloy. This is achieved through an ultrasonic assisted stir casting methodology, and a pin-on-disc tribometer is used to investigate the sliding wear rate and Coefficient of Friction (COF). Vicker's microhardness tester evaluated the microhardness of the nanocomposite, revealing it to be 18% harder than the Al 6061 alloy. Further, the metallurgical examination done through Hi-Resolution Scanning Electron Microscope (HRSEM) and X-ray diffraction (XRD) techniques confirmed the existence of SiC and B_4C nanoparticles. The wear experiment was done under diverse input wear experiment variables such as applied load, sliding velocity, and sliding distance, and optimization was done through Taguchi's technique. Applied load contributed 40.9% to wear rate, and increasing load increased wear rate due to higher pin-counter disc contact pressure. Sliding speed contributed 42.18% to the COF, while increasing it decreased it due to lower pin-disc contact. The worn area inspection revealed an abrasive wear mechanism with substantial surface degradation at higher loads. The study may progress science and develop stronger materials for many purposes.

Keywords: *hybrid nanocomposite; ultrasonic assisted stir casting methodology; wear rate; COF; Taguchi technique*

INTRODUCTION

Advancements in technology have created high-strength materials for better uses. To increase strength in low-density materials, ceramic particles are added to the Al matrix, improving mechanical qualities. Al matrix composites are widely used in aircraft, structural, ordnance, and automotive sectors due to their high specific strength, stiffness, wear, corrosion, creep, and thermal stability [1,2]. Al composites can be made using liquid or powder

Received: 2024.08.27; Received in revised form: 2024.10.21; Accepted: 2024.11.17

metallurgical methods. The liquid approach is cost-effective and commonly utilized for composite synthesis. Stir casting is a liquid-state manufacturing technology that provides advantages such as improved matrix-particle bonding, consistent reinforcement distribution, and mass production. In Al composites, classical stir-casting is limited to microsized ceramic particles due to agglomeration in Al matrices [3]. Property improvisation in the Al composites depends heavily on the added reinforcement phase. Previously, SiC and Alumina (Al_2O_3) were commonly used for property improvement. However, advances in processing have led to the synthesis of carbides, borides, nitrides, and oxides of various metals, including Titanium Diboride (TiB_2), Zirconium Diboride (ZrB_2), Aluminum Nitride (AlN), B_4C, Titanium Carbide (TiC), and Graphite (Gr) with diverse properties [4-9].

Recently, Al nanocomposites made from synthetic nanoparticles, measuring less than 100 nm, have garnered attention due to their superior strength, high modulus, load-bearing capabilities, and thermal properties, outperforming Al composites made from micro ceramics. The nanoparticle reinforcement's smaller size and shape enhance the Al nanocomposite's stiffness and stability [10]. Nanoparticles' larger surface area makes them more susceptible to agglomerate during conventional stir-casting, resulting in uneven distribution and increased porosity. Ultrasonic-assisted stir-casting gets around problems by using the ultra-vibration unit's cavitation and acoustic streaming effects to make sure that the Al alloy is highly wettable and that nanoparticles are spread out evenly [11]. Few studies have shown that ultrasonic-assisted stir casting reduces micro porosity and refines nanocomposite microstructures. Aykut Çanakçı *et al.* [12] examined how B_4C content affects AA2024/h-BN/B_4C hybrid nanocomposites' mechanical, wear, and corrosion properties. The hybrid nanocomposite samples increased porosity and decreased relative density as B_4C content increased. The hybrid nanocomposite with 4 wt% B_4C performed better. The material has 161 HB hardness and 372 MPa ultimate tensile strength, surpassing the AA2024 matrix alloy. Kai *et al.* [13] produced an in-situ ZrB_2/AA2024 composite with variable ultrasonic vibration time ranging from 1 to 9 minutes. They found that the composite achieved its maximum tensile strength (292 MPa) and ductility (19.2%) after being subjected to ultrasonic treatment for that duration of 5 minutes. Soni *et al.* [14] conducted an investigation into the comparative responses of conventional casting methods versus those utilizing ultrasonic mixing. The composite, subjected to ultrasonic mixing, exhibited a consistent distribution of reinforcement and superior mechanical properties in comparison to the traditionally mixed composite. Rui Yang *et al.* [15] successfully synthesized ZrB_2/6061Al hierarchical nanocomposites through a direct melt reaction. The development of nanoparticle clusters was contingent upon the reactive pathway. The findings indicated that the limitation of grain growth led to a refinement of grains within these nanocomposites. Furthermore, the 2 vol.% ZrB_2/6061Al nanocomposite demonstrated a commendable equilibrium between strength and ductility. Dinesh Kumar *et al.* [16] examined the impact of nano B_4C particles on ultrasonic-squeeze-assisted stir-casting LM30 alloy. Researchers found that LM30 nanocomposites with up to 1 wt.% nano B_4C particles showed improved mechanical performance due to altered primary Silicon (Si) in the Al-Si matrix. Shayan *et al.* [17] used stir-casting methodology to fabricate AA2024 nanocomposite reinforced with Titanium Dioxide (TiO_2) nanoparticles, resulting in improved mechanical characteristics.

Lightweight hybrid Al MMCs could transform aerospace and automotive industries that need high strength-to-weight ratios. A recent study shows that Al hybrid composites outperform single reinforcements in mechanical strength and wear resistance. The use of ultrasonic squeeze-assisted stir-casting to create Al hybrid nanocomposites with multiple nano reinforcements has gained popularity among researchers. Harichandran *et al.* [18] developed AA1030 + nano B_4C + nano hBN utilizing an ultrasonic stir-casting technique. The results made it clear that the ultra-vibration effect broke up the nanoparticle clusters, which led to a 40% increase in the ultimate tensile strength compared to the monolithic Al alloy material. Shayan *et al.* [19] conducted the synthesis of AA2024-nano TiO_2+nano Silicon Dioxide (SiO_2) hybrid Al nano composites through a stir-casting methodology. The findings demonstrated that the incorporation of nanoparticles led to a reduction in grain size and an enhancement of mechanical properties. Poovazhagan *et al.* [20] fabricated an Al alloy nanocomposite reinforced with SiC and B_4C nanoparticles through an ultrasonic-assisted stir casting methodology. The research concluded that the nanocomposite with 1.5 wt.% SiC and 0.5 wt.% B_4C nano particles produced the enhanced hardness properties. Vishal Kumar *et al.* [21] studied dry sliding wear in a stir-cast nano fly ash and yttrium oxide hybrid-reinforced Al 6061 nanocomposite. The microstructural study showed homogeneous reinforcing particle distribution. The nanocomposite with the most fly ash and yttrium oxide had 136% higher microhardness than the base alloy. This is because the reinforcement particles were better at holding weight. Emre Özer *et al*. [22] examined the impact of hybrid reinforcement (nano-Al_2O_3 and MWCNT) and heat treatment on the wear behavior of Al–4Cu nanocomposites. This was conducted under dry sliding conditions against a W–6Co ball using a ball-on-disk type tribometer. Furthermore, augmenting the hybrid reinforcement quantity significantly reduced the wear loss of the aged nanocomposites, leading to a state of mild wear.

The motivation for this research stems from the increasing demand for lightweight, high-strength materials in industries. Hybrid nanocomposites offer exceptional mechanical and thermal properties, making them suitable for these applications. This forms the foundation for the current study. Therefore, this effort provides a comprehensive experimental investigation of the wear behaviour experiment applied to a hybrid composite consisting of Al 6061 alloy with 0.6 vol.% SiC and 0.2 vol.% B_4C nanoparticles. The mechanical and microstructural features of the fabricated hybrid nanocomposites were evaluated. The main focus is to evaluate the optimum sliding wear variables, specifically to get the minimum wear rate and COF. The influence of the highest significant wear variable on the wear rate and COF were examined. The worn out surface performance was analyzed using HRSEM to determine the effects of different wear experiment variables.

MATERIALS AND METHODS

Materials

The matrix material was an Al 6061 alloy with the properties of a density of 2.7 g/cm^3, a tensile strength of 310 MPa, and a modulus of elasticity of 70 GPA. Magnesium (Mg) and Si are the primary alloying constituents in this precipitation-hardened Al alloy. It finds extensive use in the aerospace, maritime, and automotive sectors. The reinforcing material was a combination of nanosized SiC (3.21 g/cm^3) and B_4C (2.52 g/cm^3) particles and was purchased from Nano Research Lab, Jharkhand, India. The reinforcing particles had an average particle size of 60 nm. B_4C is a versatile reinforcing material that may be utilized with many matrix materials due to its low density and abrasion durability. However, its high cost has limited its widespread use. SiC is commonly used as reinforcement due to its reduced cost compared to B_4C.

Fabrication

The hybrid nanocomposite was created using an innovative ultrasonic cavitation technique. A resistive furnace was used to melt the 2 kg of Al 6061 alloy, which was then choked for around 10 minutes at a temperature of 680°C. The Al was protected from oxidation by a continuous flow of argon gas. Before adding the reinforcement mixture with the required proportion, the Al alloy melt was mechanically agitated at 300 rpm for 20 minutes to ensure a uniform blend. Figure 1(a) shows the mechanical stirring process. After the addition of nanoparticles in the Al melt, the primary dispersion of nanoparticles was achieved by maintaining mechanical stirring. The stirrer was then pulled out of the molten substance, and the ultrasonic horn was immersed.

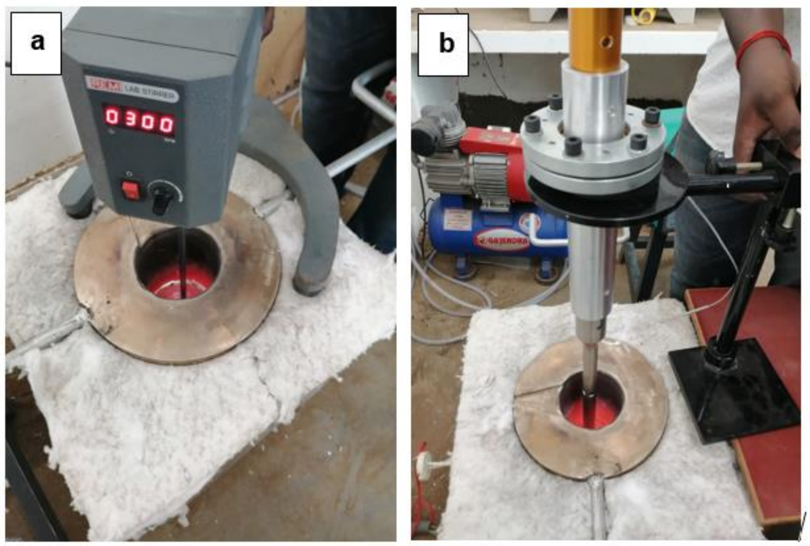

Fig. 1. Electric resistance furnace with (a) mechanical stirring setup; (b) Ultrasonic wave generating transducer

Fig. 2. Fabricated Al MMC reinforced with hybrid SiC and B_4C nanoparticles

The Titanium (Ti) ultrasonic probe was submerged in the molten material to a depth of roughly 30 mm. The ultrasonic-assisted equipment features a transducer with a constant frequency of 20 kHz and a rated power of 2 kW. The ultrasonic processing ON and OFF timings for each pulse were 1 and 0.5 seconds, respectively. Figure 1(b) shows the ultrasonication process performed on the Al nanocomposite reinforced with SiC and B_4C nanoparticles. The ultrasonic probe was taken out after processing the melt with ultrasonic waves for around 20 minutes. The steel mould (150 mm x 100 mm x 15 mm) was heated to 250°C, and the molten metal was poured into it. Figure 2 displays the fabricated Al 6061 composite reinforced with hybrid SiC and B_4C nanoparticles.

Mechanical and microstructural characterization

The fabricated Al 6061 composite reinforced with hybrid SiC and B_4C nanoparticles was tested for Vicker's microhardness using the ASTM-E384 standard with a 100 gf load for 15 seconds. Tests were conducted at five distinct locations on the specimens to disprove the chances of the indenter coming into contact with rigid ceramic particles. An average of five measurements determined Vicker's microhardness.

The microstructure of the fabricated Al 6061 composite reinforced with hybrid SiC and B_4C nanoparticles was examined through an upright optical microscope made by Olympus. The morphology of materials was characterized using HRSEM from the make of Thermo Fisher Scientific Inc., Model Apreo 2. The phases of the Al 6061 nanocomposite reinforced with hybrid SiC and B_4C nanoparticles were analyzed through XRD (Make: BRUKER, USA).

Wear experiment

The wear resistance testing was accompanied by utilizing a pin-on-disc tribometer to simulate dry sliding. The Al 6061 hybrid composite was manufactured and then machined into pins. The factory-produced pins with a 10 mm diameter and 25 mm overall length were prepared for dry friction experimentation. The pins were put through their paces against an EN30 steel disc with a surface finish (Ra) of 2.54 µm and a hardness (HRC) of 62. The wear experiments were conducted according to ASTEM G99 standards. All the tests were run on Taguchi's L_9 orthogonal array table. The test pins were cleaned and polished with acetone and SiC-1200 grit polishing paper before being put through their paces. Throughout the wear test, the friction forces were measured and averaged. Before and after each wear test, the pin's mass was determined with 0.1 mg precision using an electronic digital weight scale. Calculations for wear rate and COF were also made using Equations (1) and (2).

$$\text{Wear Rate} = \frac{\Delta m}{\rho L}\ \text{mm}^3/\text{mm} \tag{1}$$

$$\text{COF} = \frac{F_t}{F_n} \tag{2}$$

Where, Δm = Loss of weight in N, ρ = Density in g/mm^3, L = Sliding distance in mm, F_t = Tangential load in N, and F_n = Normal load in N. Table 1 summarises the wear experiment variables and three levels of the wear experiment variables. These wear experiment variables and their levels were found based on the literature and the tribometer working conditions.

***Table 1**. Wear experiment variables and their levels*

S. No	Wear experiment variables	Level -1	Level -2	Level -3
1	Applied load (N)	10	15	20
2	Sliding speed (m/s)	1	1.5	2
3	Sliding distance (mm)	1000	1500	2000

RESULT AND DISCUSSION

Hardness

Table 2 demonstrates the Vicker's microhardness values of the purchased Al 6061 alloy and the fabricated Al 6061 alloy composite reinforced with 0.6 vol.% SiC and 0.2 vol.% B_4C hybrid nano particles.

Table 2. *Vicker's microhardness values*

Specimen	Vicker's microhardness (HV)
Al 6061 alloy	54.01
Al 6061-SiC-B_4C hybrid nanocomposite	63.795

The Al 6061 alloy composite reinforced with SiC and B_4C nano particles demonstrated higher Vicker's microhardness, which is 18% higher than the Al 6061 alloy. This could be due to the large surface area enrichment of nano SiC and B_4C particles on the Al alloy. Also, the improved hardness properties of the material are mainly due to the evenly dispersed nanoparticles. As numerous researchers have found, nano ceramic particles as reinforcement make nano MMCs harder. Venkatesh *et al.* [23] observed similar trend of higher microhardness by adding nano particles in their Al alloy reinforced SiC nanocomposite.

Metallurgical characterization

Figure 3(a) and (b) demonstrate the HRSEM image of the Al 6061 alloy composite reinforced with hybrid nano SiC (0.6 vol.%) and nano B_4C (0.2 vol.%) particles manufactured through ultrasonic assisted stir casting methodology. It demonstrated the uniform settlement of SiC and B_4C nanoparticles in the Al 6061 alloy. The minimal amount of crack formation denoted some issues during the casting process. Mohammad Alipour and Reza Eslami-Farsan [24] observed similar observation in their AA7068 alloy composite reinforced with graphene nanoplatelets.

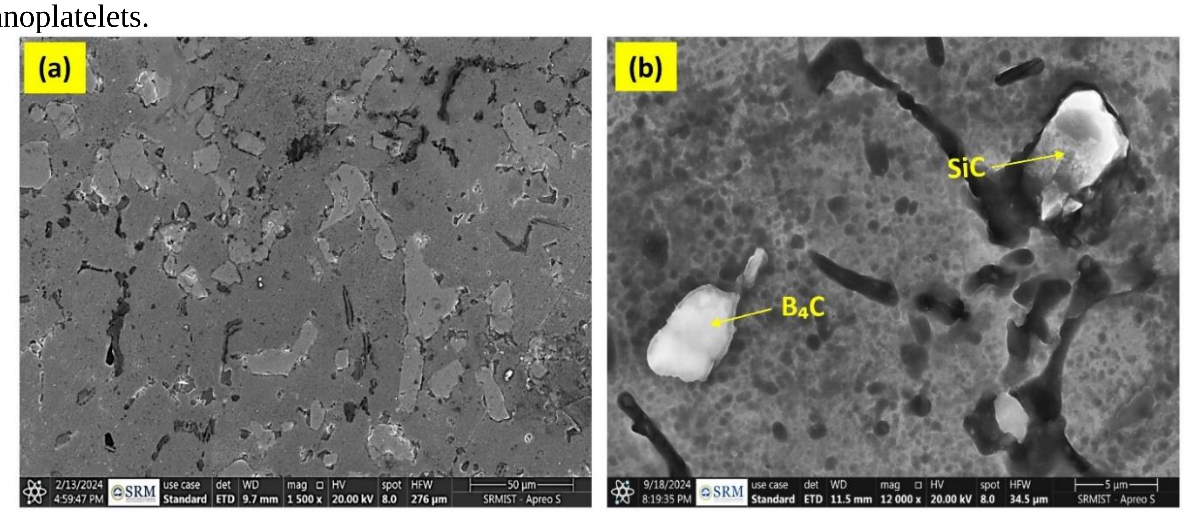

Fig. 3. (a) HRSEM image of Al composite reinforced with SiC and B_4C nanoparticles (a) at lower magnification; (b) at higher magnification

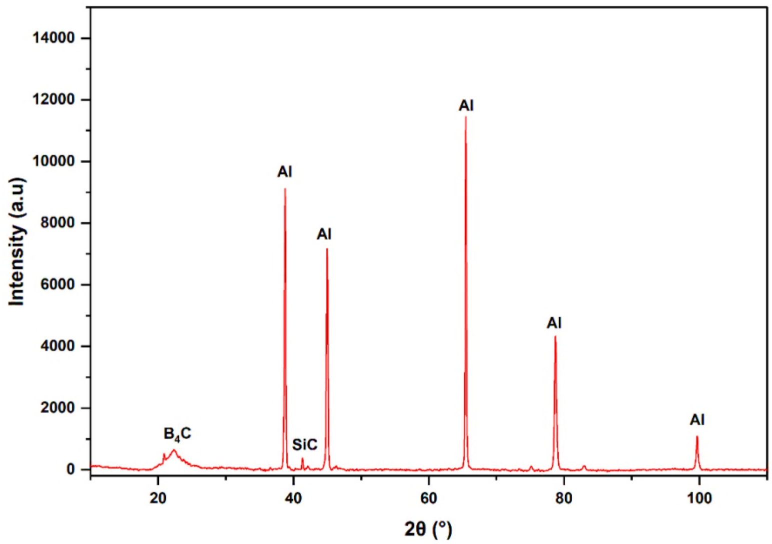

Fig. 4. XRD of Al alloy composite reinforced with SiC and B_4C nanoparticles

The XRD studies performed on the Al 6061 alloy composite reinforced with hybrid SiC (0.6 vol.%) and B_4C (0.2 vol.%) nanoparticles, confirmed the presence of Al alloy and nano reinforcement particles such as SiC and B_4C, which is proved in Figure 4. Through peaks at 2θ = 38.75°, 44.96°, 65.44°, 78.56°, and 99.67° (JCPDS card no. 89-4037), it proved the occurrence of Al. The peaks at 2θ = 41.55° (JCPDS card no. 29-1131) point out the occurrence of SiC. Additionally, for 2θ = 22.33° (JCPDS card no. 35-0798), the B_4C particles were also detected.

Influence of wear experiment variables on the wear rate

Table 3 shows the L_9 orthogonal array data with their experimental results such as wear rate and COF.

Table 3. *L9 orthogonal array wear experiment layout and its respective wear rate and COF*

Run	Applied load	Sliding speed	Sliding distance	Wear rate	COF
Unit	N	m/s	m	mm^3/m	
1	10	1	1000	1.2055 ± 0.036	0.6254 ± 0.017
2	10	1.5	1500	1.173 ± 0.035	0.6106 ± 0.018
3	10	2	2000	0.7884 ± 0.023	0.5996 ± 0.018
4	15	1	1500	1.2128 ± 0.036	0.973 ± 0.011
5	15	1.5	2000	1.2496 ± 0.037	0.5145 ± 0.015
6	15	2	1000	1.0198 ± 0.030	0.3805 ± 0.029
7	20	1	2000	1.621 ± 0.048	0.5246 ± 0.005
8	20	1.5	1000	5.1306 ± 0.153	0.4383 ± 0.013
9	20	2	1500	1.6472 ± 0.049	0.1756 ± 0.015

The log function of the target response is used as the optimization objective in the Taguchi method. Many factors of quality can be gauged using the signal-to-noise ratio. These signal-to-noise ratios reveal the sweet spot in terms of variable settings that yields the least fluctuation in response. This resulted in a reaction that was transmuted into signal-to-noise ratio. “Smaller the better” quality characteristics were utilized to perform the Taguchi’s optimization. The equation provides a "Smaller the better" solution for achieving the Signal-to-Noise ratio under the lowest wear rate conditions.

Signal-to-noise ratio (Smaller the better) = $-10 \log 1/n \,(y_1^2 + y_2^2 + \ldots\ldots + y_n^2)$ (3)

where ‘n’ is the number of measurements and ‘y_1’, ‘y_2’, ‘y_3’,…, ‘y_n’ are the values of the response. The maximum and minimum signal-to-noise ratios were shown, with the resulting delta value for the parameter indicated. The parameters with the largest delta values had the most impact on the response. The MINITAB (Version 21) statistical software was used to evaluate the results of signal-to-noise ratio and ANOVA.

Table 4 demonstrates the mean signal-to-noise ratio of the wear rate with wear experiment variables at their three levels. It was revealed that the applied load had the highest percentage of contribution to the wear rate compared to sliding velocity and sliding distance. Prathap Singh *et al.* [25] observed a similar trend of ranking in their Al alloy reinforced SiC functionally graded composite. The mean effect plot of signal-to-noise ratio for wear rate is shown in Figure 5. It shows that an applied load of 10 N, a sliding speed of 2 m/s, and a sliding distance of 2000 m are the best wear experiment variables for getting the lowest wear rate.

Table 4. *Mean signal-to-noise ratio of the wear rate*

Level	Applied load (N)	Sliding speed (m/s)	Sliding distance (m)
1	-0.3147	-2.4983	-5.3323
2	-1.2605	-5.8416	-2.4656
3	-7.5780	-0.8134	-1.3553
Delta	7.2632	5.0282	3.9770
Rank	1	2	3

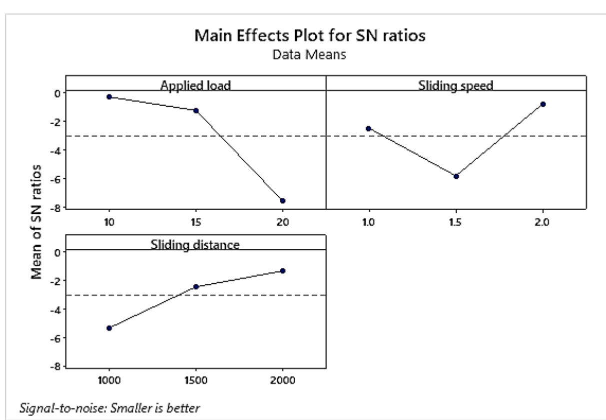

Fig. 5. Mean effect plot of signal-to-noise ratio for wear rate

Table 5. *ANOVA for the wear rate*

S. No.	Wear experiment Variables	Deg. of Freedom	Summation of square	Mean square	Contribution (%)
1	Applied load	2	5.738	2.869	40.90
2	Sliding velocity	2	3.276	1.638	23.35
3	Sliding distance	2	2.761	1.380	19.68
4	Error	2	2.252	1.126	-
5	Total	8	14.027	-	-

To learn the relative importance of each wear variable and their interactions with the response, an ANOVA was performed. Table 5 shows the ANOVA evaluated through MINITAB 21 software. The study was conducted with a 95% level of assurance and a 5% level of significance The final column of the table displays the calculated percentage contribution. Table 5 shows that the greatest contribution comes from the applied load (40.90%), followed by the sliding velocity (23.35%), and finally the sliding distance (19.68%). ANOVA analysis of wear rate confirmed that the applied load is the wear variable with the highest influence on the wear rate. Therefore, this study decided to study the influence of applied loads on the wear rate.

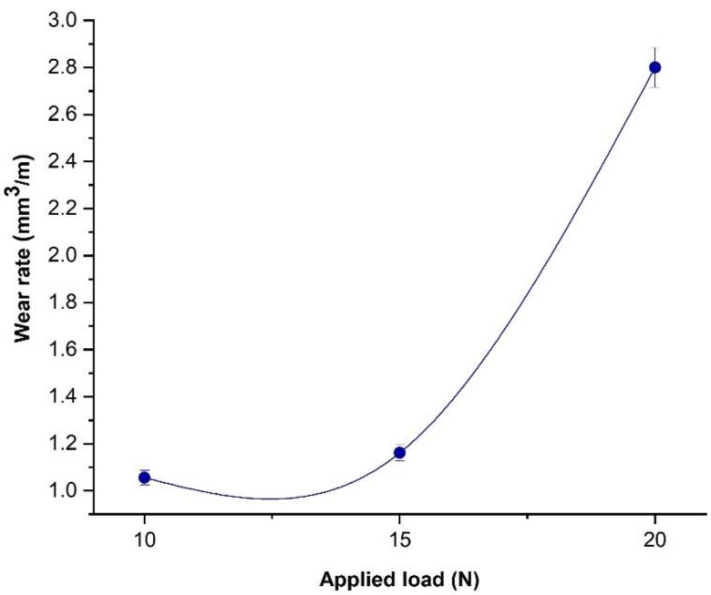

Fig. 6. Influence of applied load on the mean wear rate

The graph in Figure 6 shows how different loads change the average wear rate of the Al 6061 composite that is reinforced with SiC and B_4C nanoparticles. The graph reveals that an increase in applied load increases the wear rate of the nanocomposite. At low load conditions, the wear rate is low owing to the less contact pressure among the pin and the counter disc. Further, the increase in applied load increased the contact pressure among the pin and the counter disc, thereby increasing the wear rate. At maximum load, the wear rate reached its peak due to the high temperature generated by the increased contact pressure. Prasad Reddy *et al.* [26] found a similar trend of increasing the wear rate with the increase in the applied load in their Al 6061 alloy nanocomposite reinforced with SiC and Gr particles.

Influence of wear experiment variables on the COF

Table 6. *Mean signal-to-noise ratio of the COF*

Level	Applied load (N)	Sliding speed (m/s)	Sliding distance (m)
1	4.268	3.306	6.545
2	4.801	5.741	6.544
3	9.293	9.315	5.273
Delta	5.024	6.009	1.272
Rank	2	1	3

The "smaller the better" quality characteristics were employed for calculating the signal-to-noise ratio under conditions of minimum COF. Table 6 presented the mean signal-to-noise ratio response table for COF, demonstrating that the sliding speed, applied load, and sliding distance significantly influenced the COF. Figure 7 shows the mean effect plot for the COF. It shows that when 20 N of force is applied, sliding at 2 m/s, and going 1000 m, the COF is the lowest of all the combinations of wear experiment variables that were tested.

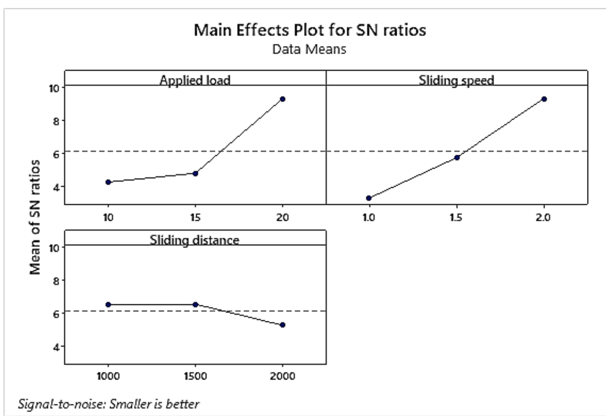

Fig. 7. Mean effect plot of signal-to-noise ratio for COF

Table 7. *ANOVA for the COF*

Sl. No.	Wear experiment Variables	Deg. of Freedom	Sum of square	Mean square	Contribution (%)
1	Applied load	2	0.11324	0.056620	30.38
2	Sliding speed	2	0.15723	0.078613	42.18
3	Sliding distance	2	0.01684	0.008421	4.52
4	Error	2	0.08543	0.042716	22.92
5	Total	8	0.37274		

Table 6 displays the results of an ANOVA conducted on the COF. Table 7 shows that the sliding velocity (42.18%) had the greatest impact on the COF, followed by the applied load (30.38%), and the sliding distance (4.52%). The ANOVA analysis of COF confirmed that the sliding velocity is the wear variable with the highest influence on the COF. Therefore, this study decided to study the influence of sliding velocity on the COF.

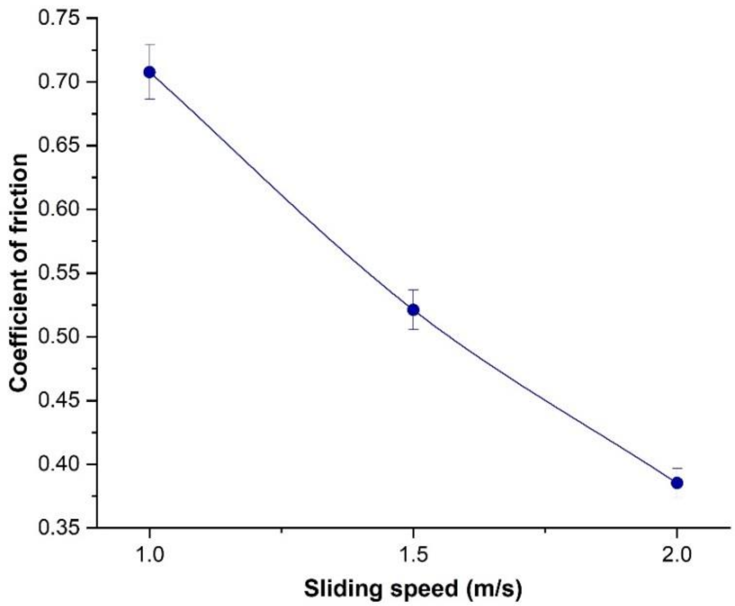

Fig. 8. Influence of sliding velocity on the mean COF

Figure 8 shows how the mean COF of the Al 6061 composite reinforced with SiC and B_4C nanoparticles changes when the sliding speed changes. The graph indicates that the nanocomposite's COF decreased as the sliding velocity increased. At lower sliding velocity (1 m/s), the COF is generally higher because of the stronger interaction between the surfaces, which results in increased adhesive forces. With an increase in sliding velocity up to 2 m/s, the COF frequently diminishes. The reason for this is that increased velocity may decrease the actual contact area between the surfaces, and the heat generated at the interface can diminish adhesive forces or cause surface imperfections to soften. As sliding velocities increase, the rise in frictional heating can lead to a higher surface temperature. The increase in temperature can cause thermal softening of the material, especially in metals and composites, which in turn leads to a decrease in the COF. Research indicates that at higher velocities, localized thermal effects may prevail, resulting in surface oxidation or material transfer, which subsequently decreases the COF. Prashant *et al.* [27] observed a similar trend of wear behavior in their Al 7075 nanocomposite, and their finding confirmed the less COF at higher velocity owing to the thermal softening.

Worn surface analysis

Figure 9 indicates the worn region of the Al 6061 alloy strengthened with hybrid SiC and B_4C nanoparticles at 10 and 20 N. The Al 6061 nanocomposite primarily displays an abrasive wear mechanism. Figure 9(a) depicts the worn exterior under minimal load conditions (10 N), displaying the typical wear tracks and demonstrating a minimal wear rate. This could be due to the reduced contact pressure between the sliding pin and the steel counter disc. Braide *et al.* [28] found that their Al alloy composite that was strengthened with carbon nanotubes and periwinkle shell nanoparticles had less surface damage when it was under minimal load.

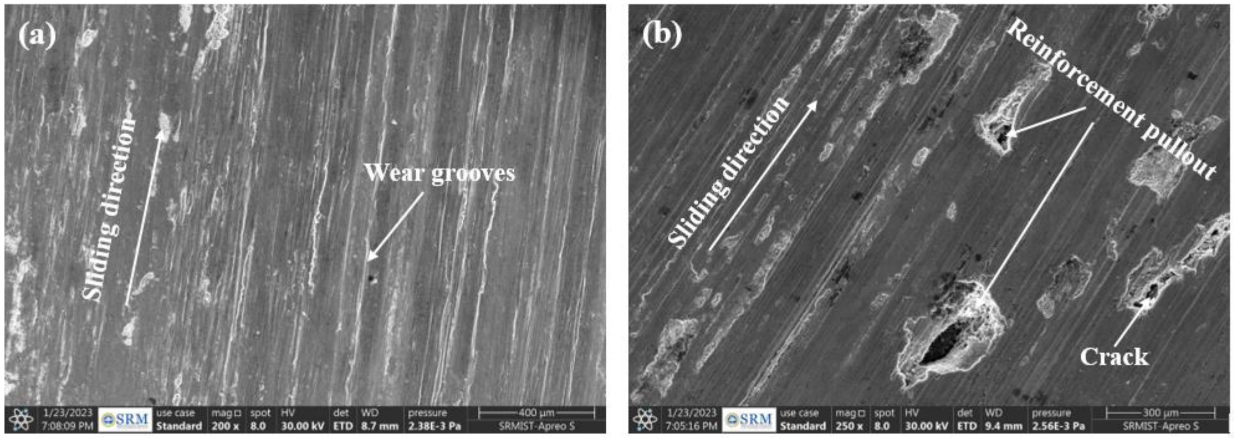

Fig. 9. Worn surface of the Al 6061 alloy composite reinforced with hybrid nanoparticles at (a) 10 N, (b) 20 N

Figure 9(b) shows the worn outside of the hybrid nanocomposite when it is under the most stress (20 N), showing major surface damage from cracks and reinforcement particle pull-out. This could be attributed to the transition from mild to severe wear. The severe wear is caused by the higher contact pressure between both sliding surfaces. Abhijit Bhowmik *et al.* [29] observed a similar trend of higher surface damage at higher load conditions in their Al alloy composite.

CONCLUSIONS

This study successfully fabricated the Al 6061 nanocomposite reinforced with hybrid 0.6 vol.% SiC and 0.2 vol.% B_4C nanoparticles using the ultrasonic-assisted stir casting method and examined their dry sliding wear performance through a pin-on-disc tribometer, leading to the following findings:

- The Vicker's microhardness test confirmed that the Al 6061 nanocomposite had an 18% higher microhardness than the Al 6061 alloy. This is because it contains hybrid SiC and B_4C nanoparticles.
- The metallurgical examination confirmed the presence of nanoparticles in the Al 6061 nanocomposite using an optical microscope and HRSEM. The XRD evaluation further confirmed the matrix and reinforcements through JCPDS cards.
- Taguchi's methodology optimized the wear rate and COF. An applied load of 10 N, a sliding speed of 2 m/s, and a sliding distance of 2000 m were sufficient to achieve the minimum wear rate. The ANOVA confirmed that the applied load, with a percentage of 40.9, was the highest contributing variable. The increase in applied load increased the wear rate. The wear rate was higher at the maximum load condition than at the lower load condition, owing to the higher contact pressure between the wear pin and the steel counter disc.
- The minimum COF was attained with an applied load of applied load of 20 N, sliding speed of 2 m/s and sliding distance of 1000 m. The ANOVA confirmed that the sliding speed, with a percentage of 42.18, was the highest contributing variable. The increase in sliding speed

decreased the COF of the nanocomposite. The COF was lower at maximum sliding speed than at minimum sliding speed, owing to the thermal softening effect.

- Finally, the worn surface examination revealed the higher surface damage at higher load conditions than lower load conditions with the observation of abrasive wear mechanisms. Aerospace applications requiring high strength with minimal self-weight can utilize the prepared hybrid nanocomposites.

Funding information: The authors declare that no funding is received to carry out this investigation.
Author contributions: All the authors have contributed to the concept, experiment, testing, analysis, and manuscript writing.
Conflict of Interest: The authors declare that they have no known competing financial interests or personal relationships that could have appeared to influence the work reported in this paper.
Data availability statement: All data generated or analyzed during this study are included in the article.

REFERENCES

1. M.K. Habibi, S.P. Joshi, M. Gupta, Hierarchical magnesium nano-composites for enhanced mechanical response. Acta Mater. 58 (2010) 6104-6114.
2. S. Tekumalla, Y. Nandigam, N. Bibhanshu, S. Rajashekara, C. Yang, S. Suwas, M. Gupta, A strong and deformable in-situ magnesium nanocomposite igniting above 1000°C. Sci. Rep. 8 (2018) 1-10.
3. S.C. Tjong, Z.Y. Ma, Microstructural and mechanical characteristics of in situ metal matrix composites. Mater. Sci. Eng. R Rep. 29 (2000) 49-113.
4. M.O. Lai, Y. Su, H.L. Teo, C.F. Feng, In situ TiB_2 reinforced Al alloy composites. Scr. Mater. 45 (2001) 1017-1023.
5. M.S. Asl, B. Nayebi, A. Motallebzadeh, M. Shokouhimehr, Nanoindentation and nanostructural characterization of ZrB_2–SiC composite doped with graphite nanoflakes. Compos. Part B (2019).
6. F.J. Haussonne, Review of the synthesis methods for AIN. Mater. Manuf. Process. 10 (1998) 717–755.
7. H. Karako, Influence of B_4C particle reinforcement on mechanical and machining properties of Al6061/B_4C composites. Compos. Part B Eng. 101 (2016) 87–98.
8. M. Hadian, H. Shahrajabian, M. Ra, Mechanical properties and microstructure of Al/(TiC+TiB_2) composite fabricated by spark plasma sintering. Ceram. Int. 45 (2019) 12088-12092.
9. S.K. Soni, D. Ganatra, P. Mendiratta, C.S.K.A. Reddy, B. Thomas, microstructure and mechanical characterization of Al_2O_3/graphene reinforced Al6061 based hybrid nanocomposites. Met. Mater. Int. 28 (2022) 545–555.
10. K. Hu, D. Yuan, S. Lu, S. Wu, Effects of nano-SiCp content on microstructure and mechanical properties of SiCp/A356 composites assisted with ultrasonic treatment. Trans. Nonferrous Met. Soc. China English Ed. 28 (2018) 2173–2180.
11. P. Madhukar, N. Selvaraj, R. Gujjala, C.S.P. Rao, Production of high performance AA7150-1% SiC nanocomposite by novel fabrication process of ultrasonication assisted stir casting. Ultrason. Sonochem. 58 (2019) 104665.

12. A. Çanakçı, A.H. Karabacak, M. Çelebi, S. Özkaya, K.A. Arpacı, A Study on the Optimization of Nano-B_4C Content for the Best Wear and Corrosion Properties of the Al-Based Hybrid Nanocomposites. Arab. J. Sci. Eng. 49 (2024) 14625–1464.
13. X. Kai, K. Tian, C. Wang, L. Jiao, G. Chen, Y. Zhao, Effects of ultrasonic vibration on the microstructure and tensile properties of the nano ZrB_2/2024Al composites synthesized by direct melt reaction. J. Alloys Compd. 668 (2016) 121–127.
14. S.K. Soni, D. Manimaran, S.B. Thomas, B. Thomas, Microstructure and mechanical characterization of Al6061 based composite and nanocomposites prepared via conventional and ultrasonic-assisted melt stirring techniques. Mater. Today Commun. 34 (2023) 105222.
15. R. Yang, Z. Zhang, Y. Zhao, G. Chen, M. Liu, L. Jiao, L. Chen, Microstructure-property analysis of ZrB_2/6061Al hierarchical nanocomposites fabricated by direct melt reaction. Mater. Char. 112 (2016) 51-59.
16. P.K. Dinesh Kumar, D.G. Solomon, Investigations on microstructure and mechanical properties on LM30-B_4C nanocomposites, fabricated through ultrasonic-squeeze assisted stir-casting. Mater Today Commun. 37 (2023).
17. M. Shayan, B. Eghbali, B. Niroumand, Fabrication of AA2024−TiO_2 nanocomposites through stir casting process. Trans. Nonferrous Met. Soc. China English Ed. 30 (2020) 2891–2903.
18. R. Harichandran, N. Selvakumar, Microstructure and mechanical characterization of (B_4C+ h-BN)/Al hybrid nanocomposites processed by ultrasound assisted casting. Int. J. Mech. Sci. 144 (2018) 814–826.
19. M. Shayan, B. Eghbali, B. Niroumand, Synthesis of AA2024-(SiO_2np+TiO_2np) hybrid nanocomposite via stir casting process. Mater. Sci. Eng. A 756 (2019) 484–491.
20. P. Lakshmanan, Abrasive wear behaviour of aluminium hybrid nanocomposites produced by ultrasonication assisted casting method. Int. J. Automot. Eng. 14(3) (2017) 4561-4573.
21. V. Kumar, S. Singh, Dry sliding wear characteristics of hybrid aluminum alloy with nano-fly ash and nano-yttrium oxide. P. I. Mech. Eng. E-J. Pro, J. (2024) 1-10.
22. E. Özer, M. Ayvaz, M. Übeyli, İ. Sarpkaya, Effect of Heat Treatment and Reinforcement Content on the Wear Behavior of Al–4Cu/Al_2O_3–CNT Nanocomposites. Arab. J. Sci. Eng. 49 (2024) 14911–14926.
23. R. Venkatesh, K. Logesh, S. Singh, P.K. Singh, I. Hossain, V. Mohanavel, M.E.M. Soudagar, S.A. Alharbi, S. Al Obaid, Aluminium alloy nanocomposite made with SiC via ultrasonic stir casting: behaviour study. J. Mech. Sci. Technol. 38 (2024) 4145-4151.
24. M. Alipour, R. Eslami-Farsani, Synthesis and characterization of graphene nanoplatelets reinforced AA7068 matrix nanocomposites produced by liquid metallurgy route. Mater. Sci. Eng. A, 706 (2017) 71-82.
25. S.P. Singh, K.A.V. Geethan, D. Elilraja, T. Prabhuram, J.I. Durairaj, Optimization of dry sliding wear performance of functionally graded Al6061 / 20% SiC metal matrix composite using Taguchi method. Mater. Today Proc. 22(4) (2020) 2824-2831.
26. A. Prasad Reddy, P. Vamsi Krishna, R.N. Rao, Tribological Behaviour of Al6061–2SiC-xGr Hybrid Metal Matrix Nanocomposites Fabricated through Ultrasonically Assisted Stir Casting Technique. Silicon, 11 (2019) 2853–2871.

27. P.S. Tile, B. Thomas, Effect of load, sliding velocity, and reinforcements on wear characteristics of Al7075-based composite and nanocomposites fabricated by ultrasonic-assisted stir-casting technique, Inter. Metalcast 18 (2024) 180–195.

28. T.K. Braide, C.C. Nwobi-Okoye, V.C. Ezechukwu, Taguchi-Grey multi-response optimization of wear parameter of new nanocomposite formulation of Al–Si–Mg alloy reinforced with synthesis carbon nanotube and periwinkle shell nanoparticles. Int. J. Adv. Manuf. Technol. 120 (2022) 8363–8375.

29. A. Bhowmik, S. Dey, D. Dey, A. Biswas, Dry Sliding Wear Performance of Al7075/SiC Composites by Applying Grey-Fuzzy Approach. Silicon 13 (2021) 3665–3680.